IUST
Iran University of Science and Technology

Iranian Journal of Electrical and Electronic Engineering

Journal Homepage: ijeee.iust.ac.ir

Design and Performance Analysis of Fuzzy Logic Controller for Solar Photovoltaic System

Kumuthawathe Ananda-Rao*(C.A.), Steven Taniselass **, Afifah Shuhada Rosmi*, Aimi Salihah Abdul Nasir*, Nor Hanisah Baharudin* and Indra Nisja***

Abstract: This study presents a Fuzzy Logic Controller (FLC)-based Maximum Power Point Tracking (MPPT) system for solar Photovoltaic (PV) setups, integrating PV panels, a boost converter, and battery storage. While FLC is known for its robustness in PV systems, challenges in battery charging and discharging efficiency can affect performance. The research addresses these challenges by optimizing battery charging, preventing overcharging, and enhancing overall system efficiency. The FLC MPPT system is designed to regulate the battery's State of Charge (SOC) while evaluating system performance under varying solar irradiance and temperature conditions. The system is modeled and simulated using MATLAB/Simulink, incorporating the PV system, MPPT algorithm, and models for the PV module and boost converter. System efficiency is assessed under different scenarios, with results showing 97.92% efficiency under Standard Test Conditions (STC) at 1000 W/m² and 25°C. Additionally, mean efficiencies of 97.13% and 96.13% are observed under varying irradiance and temperature, demonstrating the effectiveness of the FLC MPPT in regulating output. The system also extends battery life by optimizing power transfer between the PV module, boost converter, and battery, ensuring regulated SOC.

Keywords: Battery, Fuzzy Logic Controller (FLC), MATLAB/Simulink, Maximum Power Point Tracking (MPPT), Solar Photovoltaic (PV).

1 Introduction

SOLAR Photovoltaic (PV) technology presents a promising solution to meet rising energy demands while reducing greenhouse gas emissions compared to other Renewable Energy (RE) sources. This is due to its ubiquity, environmental friendliness, vast availability, and sustainability [1], [2]. However, the non-linear nature of PV systems, where output varies with changing load, temperature, and irradiation [3], presents challenges in maintaining optimal performance. Specifically, there is only one point along the power-voltage characteristic curve where the PV cell operates at maximum capacity. Consequently, a specialized control algorithm is required to continuously track this Maximum Power Point (MPP) and enhance the performance of solar PV systems [4].

Fuzzy Logic Controllers (FLCs) have gained attention for their effectiveness in managing complex and non-linear systems, including solar PV setups. By utilizing linguistic variables and fuzzy rules, FLCs emulate human decision-making processes, making them well-suited for controlling solar PV systems under varying environmental conditions. These controllers can optimize power generation, improve Maximum Power Point Tracking (MPPT), mitigate shading effects, and enhance system responsiveness to dynamic changes in solar irradiance and temperature [5], [6]. Traditional control methods, such as PID controllers, have struggled with the inherent non-linearities of PV systems [7]. To

Iranian Journal of Electrical & Electronic Engineering, 2025.
Paper first received 30 Dec 2024 and accepted 22 Feb 2025.
* The authors are with the Faculty of Electrical Engineering & Technology, University Malaysia Perlis (UniMAP), 02600 Arau, Perlis, Malaysia.
E-mails: kumuthawathe@unimap.edu.my, afifahshuhada@unimap.edu.my, aimisalihah@unimap.edu.my, norhanisah@unimap.edu.my.
** The author is with the Faculty of Electronic Engineering & Technology, University Malaysia Perlis (UniMAP), 02600 Arau, Perlis, Malaysia.
E-mail: steven@unimap.edu.my.
*** The author is with the Department of Electrical Engineering, Faculty of Industrial Technology, Bung Hatta University, Padang, West Sumatera, Indonesia.
E-mail: drindra765@bunghatta.ac.id.
Corresponding Author: Kumuthawathe Ananda-Rao.

overcome these limitations, researchers have explored intelligent control techniques, including fuzzy logic control, neural networks, and genetic algorithms, with recent studies showing promising results for FLCs in real-time control of solar PV systems [8], [9].

Several comparative analyses have been conducted to evaluate the effectiveness of FLC-based MPPT systems. Pavithra et al., [10] performed a comparative study between Perturb and Observe (P&O) and FLC-based MPPT systems using a modified SEPIC converter in MATLAB/Simulink. Their findings indicated that FLC-based MPPT controllers exhibited superior dynamic performance, reduced oscillations, higher tracking speed, and maximized power generation under different irradiation conditions. Similarly, Hayder et al., [11] compared FLC and Particle Swarm Optimization (PSO) MPPT techniques under varying solar irradiance and temperature conditions, concluding that FLC was the preferred method due to its rapidity, simplicity, and accuracy.

Further, Naureen et al., [12] conducted a comparative analysis of P&O and FLC-based MPPT methods for bifacial PV modules, which can generate more power than conventional solar panels. Their study demonstrated that FLC provided better control over panel power output, producing a stable and non-oscillating output, and enhanced the bifacial module's overall effectiveness. Azmi et al., [13] also designed an FLC-based MPPT system tailored to Malaysia's climate, showing superior MPP tracking and faster convergence speeds, though they recommended increasing the number of variables for fuzzy rules to improve control accuracy.

Additionally, Kumar Manas et al., [5] developed an FLC MPPT controller for a solar PV system, focusing on conventional, quadratic, and double-cascade boost converters, though they faced challenges with real-world validation and system hardware complexity. Sunkara Kumar et al., [14] designed a modified differential step grey wolf controller with an adaptive fuzzy logic system to handle rapid changes in sunlight intensity. Their simulations indicated higher power production at constant irradiation and reduced power as irradiation decreased. Furthermore, Abu Sayem et al., [15] integrated FLC with the Backtracking Search Algorithm (BSA) to enhance MPPT efficiency in solar car charging systems, though the added complexity raised concerns about processing time and resource utilization.

In another study, Haseeb et al., [16] employed FLC in a single-stage grid-connected PV system to enhance power quality, significantly reducing total harmonic distortion (THD) in the direct power control (DPC) of a three-phase voltage source inverter (VSI). Bouguerra et al., [17] proposed a unique MPPT algorithm based on fuzzy logic, comparing its performance with Incremental Conductance (IncCond) and Sliding Mode Controller (SMC) methods. Their findings demonstrated that the proposed FLC-based MPPT outperformed conventional techniques, responding more quickly to PV system changes and operating stably without fluctuations around the MPP.

This study aims to design and integrate an FLC-based MPPT system with a boost converter and lead-acid battery output. Unlike previous research, this study focuses on using FLC to monitor the battery's State of Charge (SOC), thereby extending battery life similarly to Pulse Width Modulation (PWM) controllers. While MPPT controllers generally outperform PWM controllers in solar power system output, they often fall short in battery life extension [18]. Additionally, the designed FLC MPPT algorithm will be analyzed under varying solar irradiance and temperature conditions.

2 Methodology

Fig. 1 illustrates the overall block diagram of the FLC based MPPT system. The solar module converts solar energy into electrical energy, with the PV link serving as the connection between the solar module and the FLC MPPT. The FLC MPPT receives current and voltage inputs from the solar PV module, which it uses to make decisions and manage the system's operation. A boost converter is integrated into the PV link to control and optimize the voltage output from the PV module, elevating it to a suitable level for charging the battery. The Pulse Width Modulation (PWM) generator is connected to the FLC MPPT, receiving the necessary control signals, specifically the duty cycle, which governs the operation of the boost converter. The duty cycle controls the power flow within the boost converter by adjusting the switching mechanism, thereby modifying the power delivery to the DC load, which, in this case, is the battery. This configuration ensures efficient power transfer from the PV system to the battery, maximizing system efficiency.

2.1 PV Module Selection

In this study, the Kyocera Solar KC200GT module was selected, with its parameters presented in Table 1. The maximum power, voltage, and current produced by this PV panel are 200.143 W, 26.3 V, and 7.61 A, respectively. The characteristics of the PV module used in this design were derived from the MATLAB/Simulink block set.

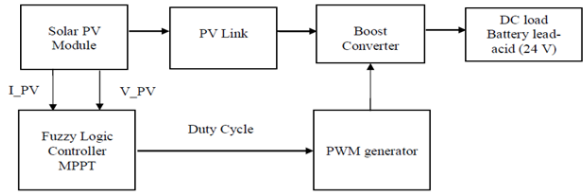

Fig 1. Overall block diagram of FLC MPPT.

Table 1. Kyocera Solar KC200GT module parameters.

Parameter	Value
Maximum Power, $\mathbf{P_{max}}$	200.143 W
Cell per module, (Ncell)	54
Open Circuit Voltage, $\mathbf{V_{OC}}$	32.9 V
Open Circuit Voltage, $\mathbf{I_{SC}}$	8.21 A
Voltage at Maximum Power Point, $\mathbf{V_{mp}}$	26.3 V
Current at Maximum Power Point, $\mathbf{I_{mp}}$	7.61 A

2.2 Boost Converter Design

Fig. 2 shows the DC-DC boost converter circuit designed for this study. The converter operates at a frequency of 25 kHz, with a peak-to-peak ripple voltage of 0.2% and an inductor current ripple of 40%. The peak-to-peak ripple voltage indicates the fluctuation in the output voltage of the PV module.

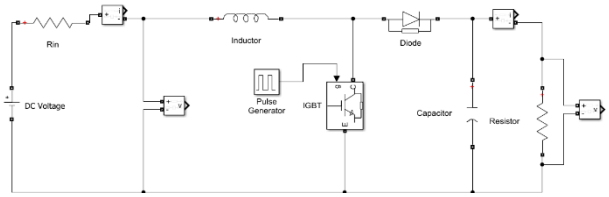

Fig 2. Boost converter circuit design.

L_{min} of the boost converter is calculated by using the formula in Eq. (1), where L_{min} is minimum inductance, V_{mp} is voltage MPP, $D_{mp(min)}$ is minimum duty cycle limit, ΔI_o is inductor current ripple factor and f_{sw} is switching frequency.

$$L_{min} = \frac{V_{mp} D_{mp(min)}}{2\Delta I_o f_{sw}} \quad (1)$$

The minimum input capacitance, $C_{i(\text{min})}$ of the boost converter is calculated by using the formula in Eq. (2). The value for MPP voltage ripple factor, ΔV_I is set at the smallest value, 0.2 % to ensure the closest optimum search by the MPPT converter.

$$C_{i(\text{min})} = \frac{4V_{mp} D_{mp(max)}}{\Delta V_I R_{in} f_{sw}} \quad (2)$$

where $C_{i(\text{min})}$ is minimum input capacitor, ΔV_I is MPP voltage ripple factor, V_{mp} is voltage MPP, $D_{mp(max)}$ is maximum duty cycle limit, R_{in} is input resistance and f_{sw} is switching frequency. The minimum output capacitance, $C_{o(\text{min})}$ of the boost converter is calculated by using the formula in Eq. (3). The output voltage ripple factor, ΔV_o is set at 0.2 %.

$$C_{o(\text{min})} = \frac{2V_o D_{mp(max)}}{\Delta V_o R_o f_{sw}} \quad (3)$$

where $C_{o(\text{min})}$ is minimum input capacitor, ΔV_o is MPP voltage ripple factor, V_{mp} is voltage MPP, $D_{mp(max)}$ is maximum duty cycle limit, R_o is output resistance and f_{sw} is switching frequency. Table 2 presents the parameters for the boost converter, calculated using Eq. (1-3).

Table 2. Parameter of boost converter.

Parameter	Value
Switching frequency	25 kHz
Inductor	2 mH
Input capacitor	1600 μF
Output capacitor	250 μF

2.3 FLC MPPT Design

The FLC MPPT algorithm was selected for this study due to its ability to effectively manage the nonlinearity of the PV system. The FLC MPPT algorithm typically follows several key steps. First, it involves measuring solar irradiance and temperature, which are critical factors influencing the power output of the PV system. These measurements serve as inputs to the algorithm. Next, the measured values of solar irradiance and temperature undergo fuzzification, where they are converted into linguistic variables. Fuzzy rules are then applied to determine the necessary adjustments to the solar panel's operating point [19], [20]. Within the FLC MPPT framework, the error (E) and the change in error (CE) at a specific sample time (k) are commonly used as significant inputs to the algorithm. These are defined by Eq. (4-5) [21], [22].

$$E(k) = \frac{P(k) - P(k-1)}{V(k) - V(k-1)} \quad (4)$$

$$CE(k) = E(k) - E(k-1) \quad (5)$$

where (E) is the error and (CE) is the change in error at a specific sample time (k). Then, P(k) is power at a specific sample time (k), and V(k) is voltage at a specific sample time (k).

In this study, the FLC MPPT process begins with the measurement of current and voltage from the PV panel, followed by the calculation of power, ΔP (change in power), ΔV (change in voltage), error (E), and change in error (CE). These calculated values are then converted into fuzzy sets. Fuzzy rules are designed to determine the output, specifically the duty cycle, based on these fuzzy sets. Table 3 presents the FLC rules used in this research, where the input variables are represented by E and CE, and the output variable is the duty cycle. The data in the table is transformed into linguistic variables using the fuzzification method. The linguistic variables include NB (negative big), NS (negative small), Z (zero), PS (positive small), and PB (positive big) [19]. Subsequently, the fuzzy output undergoes defuzzification, converting it into a precise value for the system's duty cycle [23]. This entire process is implemented using MATLAB/Simulink.

Table 3. FLC rules for FLC MPPT.

E \ CE	NB	NS	ZE	PS	PB
NB	PS	PB	NB	NB	NS
NS	PS	PS	NS	NS	NS
ZE	ZE	ZE	ZE	ZE	ZE
PS	NS	NS	PS	PS	PS
PB	NS	NB	PB	PB	PS

Fig. 3 illustrates the Simulink block diagram for the FLC MPPT circuit, detailing the process of measuring PV voltage, current, and power. The PV voltage is first input into a subtract block, which computes the difference between the current and previous voltage values. Simultaneously, the product block calculates the difference between the current and previous power values. These differences are then divided using a divide block to generate the error (E), which serves as a measure of the system's performance. The error is stored in a memory block, and the change in error (CE) is subsequently calculated. The resulting output is then passed through a saturation block to ensure it remains within desired limits. Finally, the filtered output is fed into the PWM generator (DC-DC) block for controlling the duty cycle of the system.

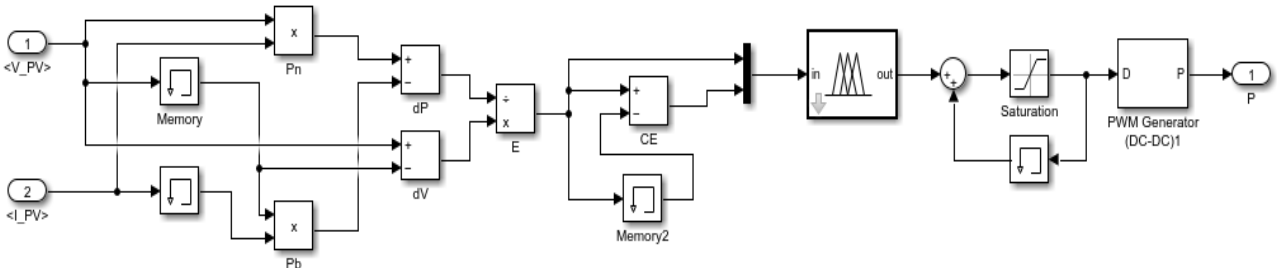

Fig 3. MPPT design in block Simulink for FLC.

2.4 Battery Model Design

Fig. 4 illustrates the charging and discharging model for a 24 V lead-acid battery. The *ChargingOn* tag is associated with two breaker blocks that govern the flow of voltage and current from the boost controller to the battery, thereby regulating the charging process. Concurrently, the *LoadOn* tag is connected to another set of breaker blocks that are responsible for linking the load with a 3Ω resistor, facilitating the discharge of the battery to power the load. The activation and deactivation of these breaker blocks, controlled by the *ChargingOn* and *LoadOn* tags, effectively manage the charging and discharging cycles of the battery system. This mechanism ensures that the power flow is optimized for efficient charging and discharging, in alignment with the solar PV system's operational requirements.

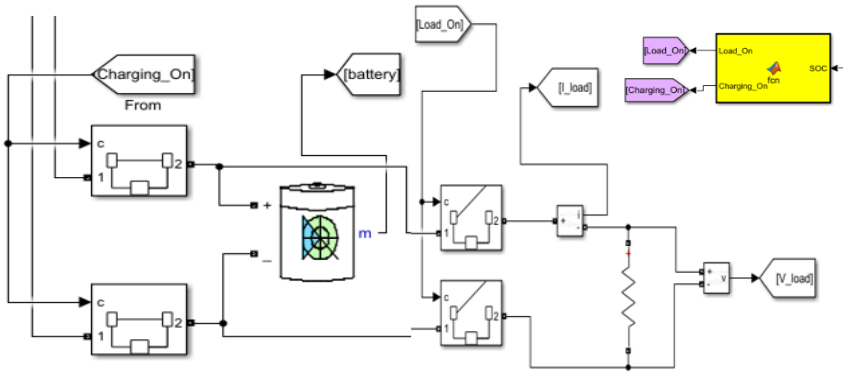

Fig 4. Battery charging/discharging switch to load model.

2.5 Overall Simulink Model

Fig. 5 presents the overall Simulink model of a standalone PV system incorporating a FLC MPPT algorithm and a boost converter, coupled with a 24 V lead-acid battery. The simulation uses a discrete time step of 1 µs to capture precise system dynamics. The PV module's inputs include a constant irradiance value, step irradiance, and step temperature, all of which influence

the module's output voltage and current. The PV system is configured with a single parallel string, featuring a series-connected module per string. The boost converter parameters are integrated into the simulation model, defining its operational characteristics and behaviour. This comprehensive setup enables the analysis and evaluation of the system's performance under various operating conditions. Additionally, the battery's SOC is monitored, and breakers control the connection between the boost converter and the battery.

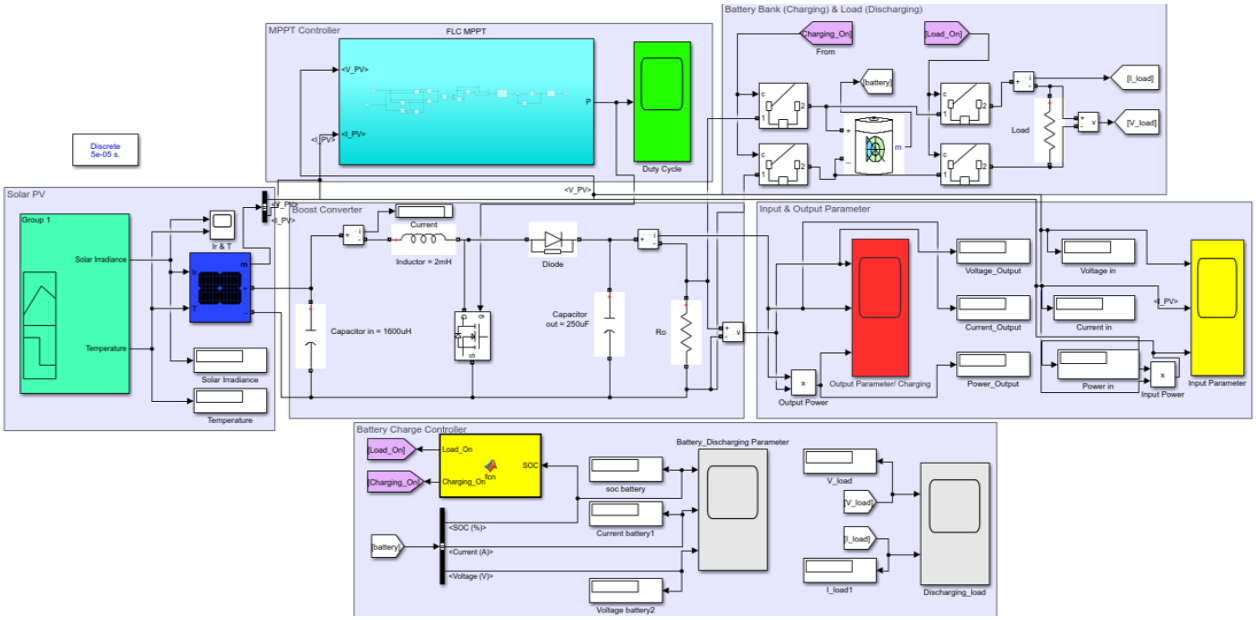

Fig 5. Overall simulink model.

3 Results and Discussion

In this study, the designed FLC MPPT algorithm was simulated to assess its performance under various conditions. Table 4 presents an analysis of the solar PV system equipped with the FLC MPPT algorithm under different solar irradiance levels. The FLC MPPT optimizes the boost converter to maintain the PV module's MPP while reducing the duty cycle percentage as irradiance increases. Additionally, Table 5 demonstrates that as the temperature rises from 25°C to 45°C, both the maximum and actual output power of the solar PV module decrease. This decrease in power output also leads to a reduction in the efficiency of the FLC MPPT algorithm, highlighting its impact on overall system performance.

Table 4. Performance analysis of FLC MPPT at varying irradiance.

Irradiance/ Temp (W/m^2) (°C)	MPP (PV Module), W	Converter Output Power, W	FLC MPPT Efficiency, $\eta MPPT$	Duty Cycle, %
100/25	19.4893	16.03	82.25%	30%
200/25	39. 9816	36.80	92.04%	15%
400/25	81.1606	74.50	91.79%	8.75%
600/25	121.79	118.0	96.89%	5%
800/25	161.503	156.0	96.59%	4%
1000/25	200.143	196.0	97.92%	3.5%

Table 5. Performance analysis of FLC MPPT at varying temperature.

Irradiance/ Temperature (W/m^2) (°C)	MPP (PV Module), W	Converter Output Power, W	FLC MPPT Efficiency, $\eta MPPT$
1000/25	200.143	196.0	97.92%
1000/35	191.495	183.5	95.82%
1000/45	182.765	173	94.66%

Fig. 6 demonstrates that the FLC MPPT exhibits a fast response time and effectively adapts to changing environmental conditions. It consistently maintains a 24 V output voltage and successfully reaches the MPP, even as the input current fluctuates with varying irradiance. As irradiance levels increase, the PV module's voltage and current also rise, dynamically adjusting the power output to align with the available solar energy. The FLC MPPT controller continuously monitors and adjusts the system's operating parameters, such as the duty cycle of the boost converter, to maintain the MPP under different irradiance conditions, as depicted in Fig. 7. Additionally, Fig. 8 illustrates the regulation of the battery storage charging current, which is determined by the available power from the solar PV module and the SOC of the battery.

Fig. 9 illustrates the FLC MPPT's quick response time and adaptability to changing environmental conditions. It efficiently maintains a 24 V output voltage and successfully reaches the MPP. As temperature increases, the PV module's voltage tends to decrease while the current tends to increase, affecting its overall power output. The FLC MPPT controller continuously monitors and adjusts the system to maintain the MPP under varying temperature conditions, as shown in Fig. 10. Although higher temperatures can slightly reduce the efficiency of the solar PV module, they generally do not cause a significant change in power output. Fig. 11 depicts the regulation of the battery storage charging current, which is determined by the available power from the solar PV module and the battery's SOC. While higher temperatures may slightly reduce the solar PV system's power output, this effect is typically less significant compared to other factors influencing system performance.

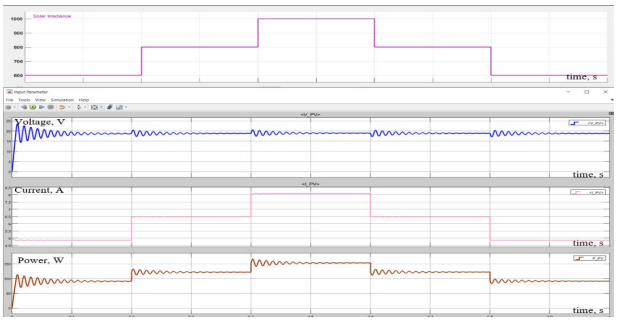

Fig 6. Solar PV output voltage(V), current (A), power (W) vs time (s) at step irradiance.

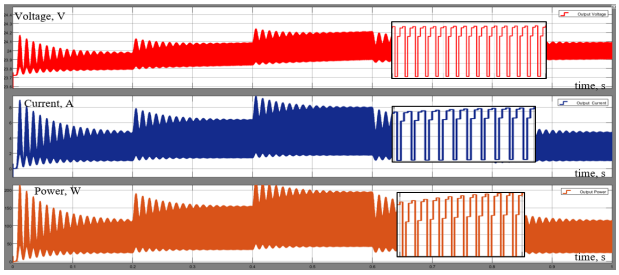

Fig 7. Boost Converter output voltage(V), current (A), power (W) vs time (s) at step irradiance.

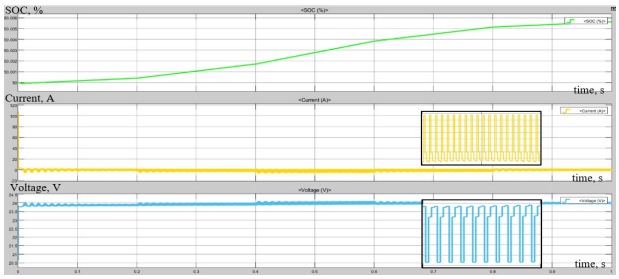

Fig 8. Changes of SOC, current (A) and voltage (V) in battery vs time (s) at step irradiance.

Next, the designed FLC MPPT controller is evaluated based on the battery's SOC and the system's switching between charging and discharging modes. When the SOC is below 20%, the battery begins charging via the PV panels. Conversely, when the SOC exceeds 80%, the battery stops charging and enters discharging mode. In Fig. 12, the battery's initial SOC is 79.9997%, indicating that it is in charging mode. However, once the SOC reaches 80%, the battery switches to discharging mode, where a decrease in battery SOC, voltage, and current can be observed. Meanwhile, Fig. 13 displays the load parameters during discharging mode. The load current increases to 8 A, and the battery voltage stabilizes at 24 V, which is due to a 3 Ω load resistance requiring 192 W for the load. The FLC MPPT then adjusts the system's output duty cycle to 3.75% in response to a solar irradiance level of 1000 W/m².

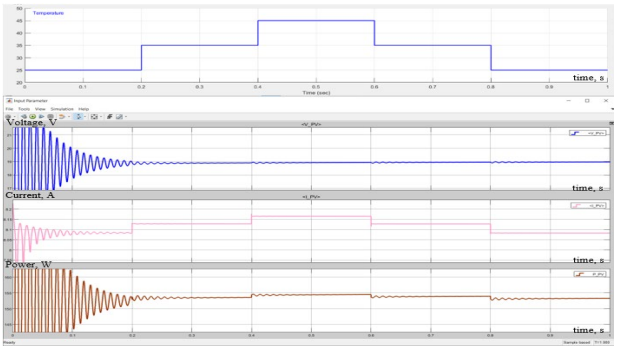

Fig 9. Solar PV output voltage(V), current (A), power (W) vs time (s) at step temperature.

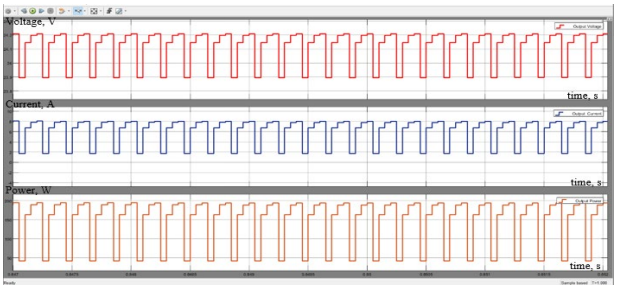

Fig 10. Boost Converter output voltage(V), current (A), power (W) vs time (s) at step temperature.

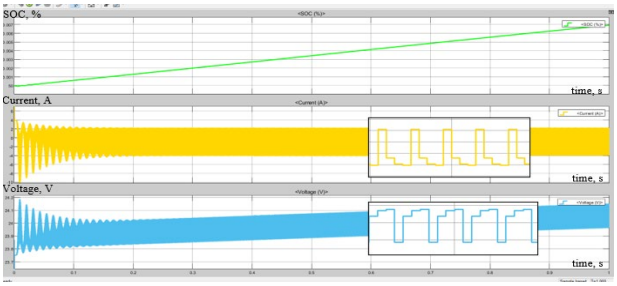

Fig 11. Changes of SOC, current (A) and voltage (V) in battery vs time (s) at step temperature.

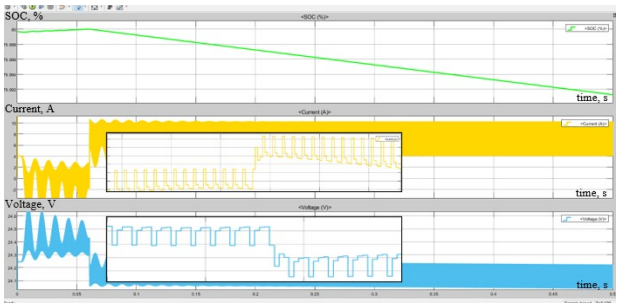

Fig 12. Initial SOC 79.9997%: Changes of SOC, Current (A) and Voltage (V) vs time (s) for constant irradiance of 1000 W/m^2.

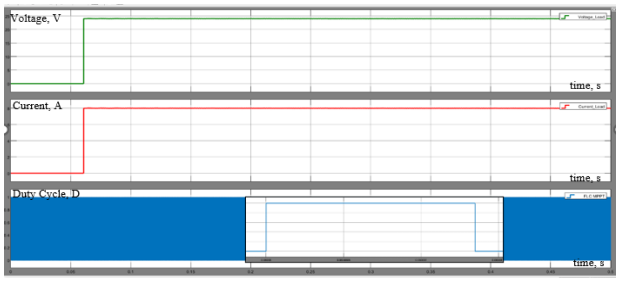

Fig 13. Initial SOC 79.9997%: Changes of Load Voltage (V), Current (A) and Duty Cycle vs time (s) for constant irradiance of 1000 W/m^2.

In Fig. 14, the battery's SOC, current, and voltage initially decrease during discharge mode. However, when the SOC reaches 20%, it begins to increase, indicating that the battery is now charging. The voltage follows a similar trend, decreasing during discharge and increasing during charging. The current remains positive during discharge mode, indicating no current is flowing into the battery, but it becomes negative during charge mode, signifying the flow of current into the battery. In Fig. 15, the load parameters during charging mode are displayed. Both the load current and voltage values are near zero, indicating no power is being supplied to the load resistance. Similarly, the FLC MPPT adjusts the system's output duty cycle to 3.75% in response to a solar irradiance level of 1000 W/m².

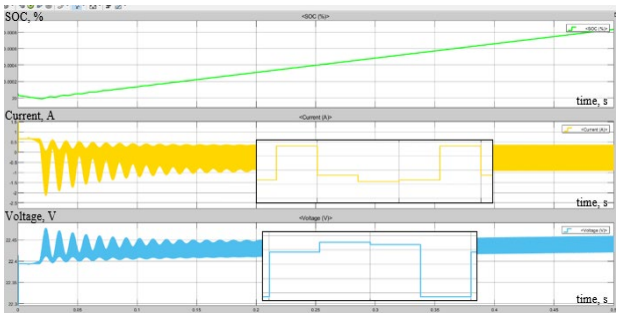

Fig 14. Initial SOC 20.00001%: Changes of SOC, Current (A) and Voltage (V) vs time (s) for constant irradiance of 1000 W/m^2.

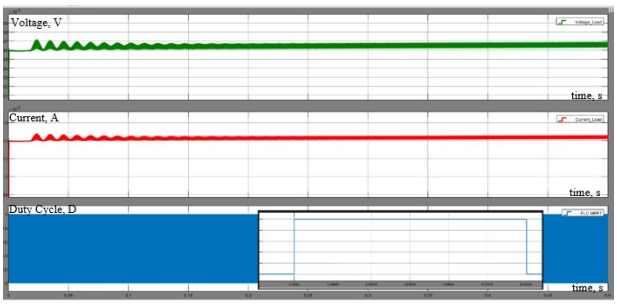

Fig 15. Initial SOC 20.00001%: Changes of Load Voltage (V), Current (A) and Duty Cycle vs time (s) for constant irradiance of 1000 W/m^2.

Overall, the integration of the FLC MPPT ensures that the battery's SOC remains within a specified range of 20% to 80%. If the SOC drops below 20% or exceeds 80%, the system triggers actions to charge or discharge the battery until it returns to the desired SOC range. This proactive approach maximizes the battery's lifetime and enhances the solar PV system's efficiency by dynamically adjusting the charging and discharging processes based on real-time SOC measurements.

4 Conclusion

In this work, a standalone PV power system integrated with a boost converter and a battery has been successfully designed, with a focus on developing an FLC MPPT algorithm to regulate the battery's SOC and extend its lifespan. By utilizing a boost converter known for its high efficiency and stability across varying duty cycles, the FLC MPPT algorithm effectively achieved MPP extraction, adapting to different irradiance and temperature levels. Simulations conducted under various conditions demonstrated the system's efficiency, achieving 97.92% under STC and maintaining mean efficiencies of 97.13% under varying irradiance and 96.13% under varying temperatures.

Additionally, the results of the battery SOC evaluation clearly demonstrate the success of extending battery lifetime through SOC regulation. When the battery SOC falls below 20%, the battery begins charging, and when the SOC exceeds 80%, the battery stops charging and enters discharging mode. Overall, the simulation results showcased the adaptability and effectiveness of the FLC MPPT system in optimizing the performance of a solar PV system, particularly in managing power output, battery lifetime, and overall system efficiency under changing environmental conditions. Nevertheless, for further performance improvement, it is recommended to incorporate a second-stage DC-DC converter with a Proportional-Integral (PI) controller and to consider PV system operations under Partial Shading Conditions (PSCs).

Conflict of Interest

The authors declare no conflict of interest.

Author Contributions

Kumuthawathe Ananda-Rao, Steven Taniselass, Afifah Shuhada Rosmi and Aimi Salihah Abdul Nasir: Conceptualization, Methodology, Result analysis and Writing.

Nor Hanisah Baharudin and Indra Nisja: Supervision, Revise and Editing.

Funding

This work is partially funded by Faculty of Electrical Engineering & Technology, Universiti Malaysia Perlis (UniMAP) under FKTE research fund and by the Centre of Excellence for Renewable Energy (CERE), Universiti Malaysia Perlis (UniMAP).

Informed Consent Statement

Not applicable.

Acknowledgment

The authors acknowledge the financial support provided by the Faculty of Electrical Engineering & Technology, Universiti Malaysia Perlis (UniMAP) under FKTE research fund and by the Centre of Excellence for Renewable Energy (CERE), Universiti Malaysia Perlis (UniMAP).

References

[1] N. Sulaiman, S. I. Ihsan, S. N. S. A. Bakar, Z. A. A. Majid, and Z. A. Zakaria, "Evacuated Tubes Solar Air Collectors: A Review on Design Configurations, Simulation Works and Applications," *Progress in Energy and Environment*, vol. 25, pp. 10–32, 2023.

[2] Z. Ilham, N. A. I. Saad, W. A. A. Q. I. Wan, and A. A. Jamaludin, "Multi-Criteria Decision Analysis for Evaluation of Potential Renewable Energy Resources in Malaysia," *Progress in Energy and Environment*, vol. 21, 2022.

[3] M. Ali, M. Ahmad, M. A. Koondhar, M. S. Akram, A. Verma, and B. Khan, "Maximum Power Point Tracking for Grid-Connected Photovoltaic System Using Adaptive Fuzzy Logic Controller," *Computers and Electrical Engineering*, vol. 110, 2023.

[4] M. Zerouali, A. El Ougli, and B. Tidhaf, "A Robust Fuzzy Logic PI Controller for Solar System Battery Charging," *Int. J. Power Electronics and Drive Syst.*, vol. 14, pp. 384–394, 2023.

[5] S. K. Manas and B. Bhushan, "Performance Analysis of Fuzzy Logic-Based MPPT Controller for Solar PV System Using Quadratic Boost Converter," *Advances in Energy Technology*, vol. 766, no. LNEE, 28, pp. 69–79, 2021.

[6] T. M. Lima and J. A. C. B. Oliveira, "FPGA-Based Fuzzy Logic Controllers Applied to the MPPT of PV Panels – A Systematic Review," *IEEE Trans. Fuzzy Syst.*, pp. 1–10, 2024.

[7] A. Daraz, B. A. Basit, and G. Zhang, "Performance Analysis of PID Controller and Fuzzy Logic Controller for DC-DC Boost Converter," *PLoS One*, vol. 18, no. 10, pp. e0281122, 2023.

[8] T. Hai, J. Zhou, and K. Muranaka, "An Efficient Fuzzy-Logic Based MPPT Controller for Grid-Connected PV Systems by Farmland Fertility Optimization Algorithm," *Optik*, vol. 267, p. 169636, 2022.

[9] A. Mutia, D. Abdullah, K. Kraugusteeliana, S. A. Pramono, and H. Sama, "Simulation of Solar Panel Maximum Power Point Tracking Using the Fuzzy Logic Control Method," *Majlesi J. Electr. Eng.*, vol. 17, no. 2, pp. 29–39, 2023.

[10] C. Pavithra, V. S. Vidhyareni, M. Vijayadharshini, S. A. K. B. Shree, and N. Varsha, "Comparison of Solar P&O and FLC-Based MPPT Controllers & Analysis Under Dynamic Conditions," *EAI Endorsed Trans. Energy Web*, vol. 11, 2024.

[11] W. Hayder, A. Abid, M. B. Hamed, E. Ogliari, and L. Sbita, "Comparison of MPPT Methods FLC & PSO for PV System Under Variable Irradiance and Temperature," in *Proc. 18th Int. Multi-Conf. Systems, Signals & Devices (SSD)*, Monastir, Tunisia, pp. 1247–1251, 2021.

[12] N. Siddiqui and M. S. Ghole, "Comparative Analysis of P&O and Fuzzy Logic Based MPPT Methods for Bi-Facial Photovoltaic Module," in *Proc. 2024 IEEE Int. Students' Conf. Electrical, Electronics and Computer Sci.*, 2024.

[13] M. H. Azmi, S. M. Noor, and S. Musa, "Fuzzy Logic Control Based Maximum Power Point Tracking Technique in Standalone Photovoltaic System," *Int. J. Power Electronics and Drive Syst.*, vol. 14, pp. 1110–1120, 2023.

[14] S. Kumar and B. K. Balakrishna, "A Novel Design and Analysis of Hybrid Fuzzy Logic MPPT Controller for Solar PV System Under Partial Shading Conditions," *Sci. Rep.*, vol. 14, 2024.

[15] S. Abu, A. Nadzirah, A. Al-Shetwi, M. A. Hannan, P. J. Ker, M. A. Rahman, and K. Muttaqi, "Fuzzy Based BSA Optimization for Maximum Power Point Tracking Controller Performance Evaluation," *IEEE Ind. Appl. Soc. Annu. Meet. (IAS)*, Vancouver, BC, Canada, pp. 1–8, 2021.

[16] M. Haseeb, A. Mansour, and E. Othman, “Enhancing of Single-Stage Grid-Connected Photovoltaic System Using Fuzzy Logic Controller,” *Int. J. Electr. Comput. Eng. (IJECE)*, vol. 14, pp. 2400–2412, 2024.

[17] K. Bouguerra, S. Latreche, and M. Khemliche, "Comparative Study Between IncCond and FLC and SMC Algorithms for MPPT Control for Grid Connected PV System," in *Proc. 2nd Int. Conf. Electr. Eng. Automatic Control (ICEEAC)*, Setif, Algeria, 2024.

[18] P. S. Acharya and P. S. Aithal, "A Comparative Study of MPPT and PWM Solar Charge Controllers and Their Integrated System," *J. Phys. Conf. Ser.*, vol. 1712, no. 1, p. 012023, 2020.

[19] B. Chandrashekar, J. Pradeep, M. M., M. Sivasubramanian, K. L. Khandan, and J. A. Dhanraj, "A Fuzzy Logic Controller for a Photovoltaic System Relying on a Closed-Loop DC-DC Converter," in *Proc. 9th Int. Conf. Sci. Technol. Eng. Math. (ICONSTEM)*, Chennai, India, pp. 1–5, 2024.

[20] K. Ananda-Rao et al., “MPPT Charge Controller Using Fuzzy Logic for Battery Integrated with Solar Photovoltaic System,” *J. Adv. Res. Appl. Sci. Eng. Technol.*, vol. 47, no. 2, pp. 171–182, 2024.

[21] S. Kaur and S. Vig, "Modeling of MPPT-Based Solar Eco-System Using Fuzzy Logic Controller," in *IOP Conf. Ser.: Earth Environ. Sci.*, vol. 1110, no. 1, p. 012079, 2023.

[22] L. K. Narwat and J. Dhillon, "Design and Operation of Fuzzy Logic Based MPPT Controller Under Uncertain Condition," *J. Phys. Conf. Ser.*, vol. 1854, no. 1, p. 012035, 2021.

[23] M. Bouksaim, M. Mekhfioui, and M. N. Srifi, “Design and Implementation of Modified INC, Conventional INC, and Fuzzy Logic Controllers Applied to a PV System Under Variable Weather Conditions,” *Designs*, vol. 5, no. 4, p. 71, 2021.

[24] R. Sharma, V. Saran, S. Kanaujia, and S. Gupta, “Evaluation of MPPT Controller Performance Using Fuzzy Logic Design with Wireless Sensor Node,” in *Proc. Int. Conf. Smart Syst. App. Electr. Sci. (ICSSES)*, 2024.

Biographies

Kumuthawathe Ananda-Rao received her B.Eng (Hons) degree in Industrial Electronic Engineering from Universiti Malaysia Perlis (UniMAP) in 2008 and Ph.D in Electrical System Engineering in 2018 from the same university. Her research interests include renewable energy, energy management system, energy storage specialized in battery energy storage system and power electronics.

Steven Taniselass received his B.Eng (Hons) degree in Microelectronic Engineering from Universiti Malaysia Perlis, (UniMAP) Malaysia in 2008, and had completed his Master of Science degree in Microelectronic Engineering in 2011. In 2021, he obtained his Ph.D. in Nano Electronic Engineering from the same university. His research interests include nanomaterials, graphene derivatives, biosensors and energy storage devices.

Afifah Shuhada Rosmi received her Bachelor of Engineering (Honours) degree in Electrical System Engineering from Universiti Malaysia Perlis (UniMAP) in 2013. She subsequently earned her Ph.D. in Electrical System Engineering from the same institution in 2018, specializing in piezoelectric energy harvesting for MEMS applications. Her current research interests include renewable energy harvesting and partial discharge monitoring and classification, with a focus on using artificial intelligence approaches.

Aimi Salihah Abdul Nasir received her B.Eng (Hons) degree in Mechatronic Engineering from Universiti Malaysia Perlis (UniMAP) in 2009. In 2015, she obtained her Ph.D. in Biomedical Electronic Engineering from the same university, specialized in medical

image processing with a focus on the clustering analysis. Her research interests include image processing, medical image analysis, artificial intelligence, and deep learning.

Nor Hanisah Baharudin received her B.Eng (Hons) degree in Electrical & Electronics from Universiti Teknologi Petronas in 2005 and M.Eng. Sc in Renewable Energy Electrical Power System from Curtin University of Technology, Australia in 2009. In 2018, she obtained her Ph.D in Electrical System Engineering from Universiti Malaysia Perlis (UniMAP). Her research interests include renewable energy system and application, power electronic converters and power system analysis.

Indra Nisja received his Ph.D. degree in electrical engineering, Universiti Sains Malaysia in 2014. He is currently a lecturer in Department of Electrical Engineering, Universitas Bung Hatta, Padang, West Sumatera, Indonesia. His research interest includes electrical power system, especially in power quality and electronic drive.